3694–3699 *Nucleic Acids Research, 1998, Vol. 26, No. 16*

Structural characteristics of 2′-*O*-(2-methoxyethyl)-modified nucleic acids from molecular dynamics simulations

Kenneth E. Lind, Venkatraman Mohan[1], Muthiah Manoharan[1] and David M. Ferguson*

Department of Medicinal Chemistry and Minnesota Supercomputing Institute, University of Minnesota, 308 Harvard Street SE, Minneapolis, MN 55455, USA and [1]ISIS Pharmaceuticals, 2922 Faraday Avenue, Carlsbad, CA 92008, USA

Received May 12, 1998; Revised May 27, 1988; Accepted June 30, 1998

ABSTRACT

The structure and physical properties of 2′-sugar substituted *O*-(2-methoxyethyl) (MOE) nucleic acids have been studied using molecular dynamics simulations. Nanosecond simulations on the duplex MOE[CCAACGTTGG]-r[CCAACGUUGG] in aqueous solution have been carried out using the particle mesh Ewald method. Parameters for the simulation have been developed from *ab initio* calculations on dimethoxyethyl fragments in a manner consistent with the AMBER 4.1 force field database. The simulated duplex is compared with the crystal structure of the self-complementary duplex d[GCGTAT$_{MOE}$ACGC]$_2$, which contains a single modification in each strand. Structural details from each sequence have been analyzed to rationalize the stability imparted by substitution with 2′-*O*-(2-methoxyethyl) side chains. Both duplexes have an A-form structure, as indicated by several parameters, most notably a C3′ *endo* sugar pucker in all residues. The simulated structure maintains a stable A-form geometry throughout the duration of the simulation with an average RMS deviation of 2.0 Å from the starting A-form structure. The presence of the 2′ substitution appears to lock the sugars in the C3′ *endo* conformation, causing the duplex to adopt a stable A-form geometry. The side chains themselves have a fairly rigid geometry with *trans*, *trans*, *gauche*+/– and *trans* rotations about the C2′-O2′, O2′-CA′, CA′-CB′ and CB′-OC′ bonds respectively.

INTRODUCTION

The structure and stability of chemically modified nucleic acids is of great importance to the design of antisense oligonucleotides. Over the last 10 years, a variety of synthetic modifications have been proposed to increase nuclease resistance or to enhance the affinity of the antisense strand for its target mRNA (1,2). While a great deal of information has been collected about the types of modifications that improve duplex formation, little is known about the structural basis for the improved affinity observed. In general, RNA:RNA duplexes are more stable or have higher melting temperatures (T_m) than DNA:DNA duplexes (3–5). The increased stability of RNA has been attributed to several structural features, most notably the improved base stacking interactions that result from an A-form geometry (6). The presence of the 2′-hydroxyl in RNA biases the sugar toward a C3′ *endo* pucker (Northern), which causes the duplex to favor the A-form geometry. On the other hand, deoxy nucleic acids prefer a C2′ *endo* sugar pucker (Southern), which is thought to impart a less stable B-form geometry (3). In addition, the 2′-hydroxyl groups of RNA can form a network of water-mediated hydrogen bonds that help stabilize the RNA duplex (7).

DNA:RNA hybrid duplexes, however, are usually less stable than pure RNA:RNA duplexes and, depending on their sequence, may be either more or less stable than DNA:DNA duplexes (4). The structure of a hybrid duplex is intermediate between the A- and B-form geometries, which may result in poor stacking interactions (8–11). The stability of a DNA:RNA hybrid is central to antisense therapies, as the mechanism requires binding of a modified DNA strand to an mRNA strand. To effectively inhibit the mRNA, the antisense DNA should have a very high binding affinity for the mRNA. Otherwise, the desired interaction between the DNA and target mRNA strand will occur infrequently, thereby decreasing the efficacy of the antisense oligonucleotide.

One of the more exciting synthetic modifications that does have increased nuclease resistance and a very high binding affinity is the 2′ sugar-substituted *O*-(2-methoxyethyl) (MOE) side chain (12,13; Fig. 1). MOE-substituted oligonucleotides have shown outstanding promise as antisense agents in several disease states and are presently being investigated in clinical trials for the treatment of CMV retinitis. One of the biggest advantages of the MOE substitution is the improvement in binding affinity, which is greater than many similar 2′ modifications, such as *O*-methyl, *O*-propyl and *O*-aminopropyl (13). The high binding affinity has been partially attributed to the 2′ substitution causing a C3′ *endo* sugar pucker, which in turn may give the oligomer a favorable A-form like geometry (13). This is a reasonable hypothesis, since substitution at the 2′ position by a variety of electronegative groups (such as fluoro and *O*-alkyl chains) has been demonstrated to cause C3′ *endo* sugar puckering (3,14). In addition, it has been

*To whom correspondence should be addressed. Tel: +1 612 626 2601; Fax: +1 612 626 4429; Email: ferguson@vwl.medc.umn.edu

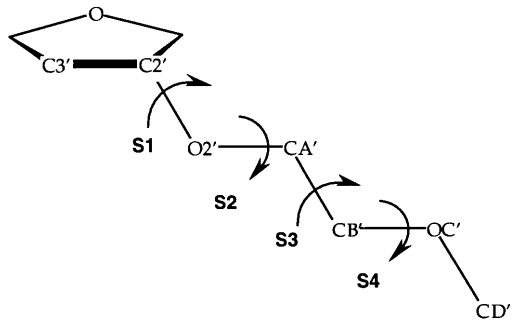

Figure 1. 2′-*O*-(2-methoxyethyl) side chain and associated torsions. S1, C3′-C2′-O2′-CA′; S2, C2′-O2′-CA′-CB′; S3, O2′-CA′-CB′-OC′; S4, CA′-CB′-OC′-CD′.

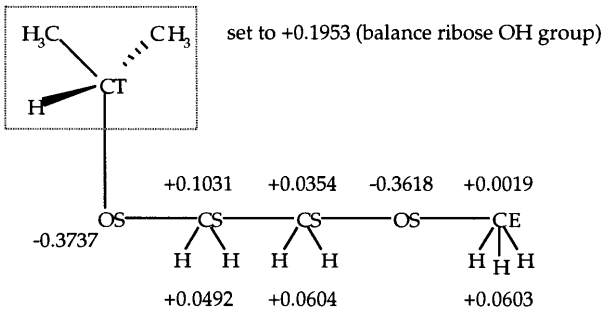

Figure 2. Partial charges and atom types for the 2-*O*-(2-methoxyethyl)propyl model.

suggested that a *gauche* interaction between the oxygen atoms around the O-C-C-O torsion of the side chain has a stabilizing effect on the duplex (13). Such *gauche* interactions have been observed experimentally for a number of years (15,16), however, their relevance for antisense applications remains speculative. It is hypothesized that this *gauche* effect results in a configuration of the side chain that is favorable for duplex formation (13). The exact nature of this stabilizing configuration has not yet been explained. It may be that holding the O-C-C-O torsion in a single *gauche* configuration, rather than the more random distribution seen in an alkyl side chain, provides an entropic advantage for duplex formation (17).

The goal of the work presented here was to examine the dynamic structural properties of 2′-modified *O*-(2-methoxyethyl) oligonucleotides. Specifically, the overall shape of the duplex, sugar pucker profile and side chain conformations were determined. The analysis and interpretation of these structural results is used to understand how this modification leads to increased duplex stability. In the initial stage, parameters for the MOE-substituted duplex are developed to be consistent with the AMBER database. A stable nucleic acid duplex is then produced from a molecular dynamics simulation utilizing the AMBER force field (18) and the particle mesh Ewald technique (19) to treat long-range electrostatic interactions. The resulting trajectory is analyzed and compared with X-ray crystallographic data to further explore the effects of the 2′ substituent on the structure and stability of the antisense complex.

PARAMETERIZATION

A 2-*O*-(2-methoxyethyl)propyl model compound was used for the development of partial atomic charges for the MOE side chain. Compatibility with the AMBER database was achieved by employing the RESP methodology (20). The Gaussian 94 program (21) was used to calculate the HF/6-31G* electrostatic potential of the MOE-propyl model compound, which was then fitted to the RESP module of the AMBER 4.1 package (22). The charge on the propyl backbone was set to balance that of the 2′-hydroxyl group of a standard ribose sugar from the AMBER database, thereby maintaining consistency among sugars. The net charge of the OH group is –0.1953, thus the propyl backbone was set to +0.1953 during the calculation.

The partial charges for the *O*-(2-methoxyethyl) fragment of the sugar are shown in Figure 2. The substituted 2′-oxygen (–0.3737) is less negative than the corresponding ribose 2′-oxygen (–0.6193). In fact, the charge on both oxygen atoms of the side chain is remarkably similar to that of the ether oxygen of the ribose sugar (–0.3548). The partial charges of the methyl and methylene groups appear to be similar to those of other hydrocarbon chains in the AMBER database.

All bond and angle terms for the side chain were taken from the current AMBER 4.1 database and did not require modification. The torsional profile around the C-C-O-C and O-C-C-O dihedrals of the side chain was re-parameterized based on *ab initio* calculations. Two new atoms were added to the database, CS for the side chain methylene carbons and CE for the terminal methyl group, as shown in Figure 2. These are identical to the standard CT atom type in AMBER, but with a different torsional profile around bonds containing oxygen. MP2/6-31G*//HF/6-31G* energies were calculated for each of the low energy conformations of a 1,2-dimethoxy ethane model fragment. For comparison, DFT calculations (B3LYP/6-31G*//HF/6-31G*) for the same fragment were also performed.

The energy profile of the 1,2-dimethoxy ethane molecule is shown in Table 1. The complete rotational profile for this molecule has been calculated by Jaffe and co-workers using a Dunning 95 basis set (23). In the current study, *gauche* rotations around the first bond were not calculated, since the presence of the sugar and phosphate backbone in the complete duplex forces a *trans* conformation for the C3′-C2′-O2′-CA′ torsion. The only possible types of rotations along the MOE side chain are *trans*/*trans*/*trans*, *trans*/*trans*/*gauche*, *trans*/*gauche*/*trans*, *trans*/*gauche*+/*gauche*+ and *trans*/*gauche*–/*gauche*+. Our *ab initio* results on these conformations are in excellent agreement with those from a similar study by Jaffe and co-workers. The lowest energy conformer has an extended *trans*/*trans*/*trans* geometry, while the *trans*/*gauche*–/*gauche*+ conformer is only 0.2 kcal higher in energy. This low energy *trans*/*gauche*–/*gauche*+ structure is of special interest as it has been observed in gas phase calculations to form an attractive 1,5 CH_3/O interaction (23). The unique O···H interaction appears to stabilize the conformer such that it is only slightly higher in energy than the extended conformer. This type of interaction may be important in the gas phase, which leads to higher populations of the conformer, but in solution the 1,5 interaction may be less pronounced. In fact, increasing the dielectric constant for gas phase calculations as a test to mimic solvent screening effects has a profound impact on the relative energies of all conformers. In a higher dielectric field, the *trans*/*gauche*/*trans* conformer has the lowest energy and the *trans*/*gauche*+/*gauche*+ and *trans*/*gauche*–/*gauche*+ conformers

are both slightly lower than the extended conformation. This agrees with NMR studies that indicate that the *trans*/*gauche*/*trans* conformer is more stable than *trans*/*trans*/*trans* by 0.4 kcal/mol in a variety of solvents (23–25).

Table 1. Torsional profile for 1,2-dimethoxy ethane

Level of Theory	Conformer Energies (kcal)[a] 1	2	3	4	5
MM2 opt	1.3522	0.1953	2.6664	1.2542	0.0000
HF/STO-G opt	2.2402	0.5791	0.7531	1.6062	0.0000
HF/3-21G opt	4.3909	2.8112	0.3067	1.5006	0.0000
HF/6-31G*//HF/STO-3G	3.4936	1.6052	1.9170	2.0919	0.0000
HF/6-31G*//HF/3-21G	3.2405	1.6270	1.8951	1.7065	0.0000
HF/6-31G* opt	3.6153	1.7800	2.0241	2.1986	0.0000
HF/6-311G*//HF/6-31G*	3.3966	1.3498	1.5610	2.0321	0.0000
MP2/6-31G*//HF/3-21G	1.9457	0.7340	0.0055	1.3336	0.0000
B3LYP/6-31G*//HF/3-21G	1.7298	0.6040	0.2646	1.2654	0.0000
MP2/6-31G*//HF/6-31G*	2.0258	0.6045	0.2098	1.5105	0.0000
MP2/6-311G*//HF/6-31G*	2.2218	0.6714	0.2068	1.6439	0.0000

[a]Conformations of 1,2-dimethoxy ethane around COCC/OCCO/CCOC torsions: 1, *trans*/*gauche*/*gauche* (actual 180.0/78.6/70.9); 2, *trans*/*trans*/*gauche* (actual 180.0/167.9/78.2); 3, *trans*/*gauche–*/*gauche+* (actual 180.0/281.1/76.2); 4, *trans*/*gauche*/*trans* (actual 180.0/85.4/178.5); 5, *trans*/*trans*/*trans* (actual 180.0/180.0/180.0).

The AMBER force field database was modified to reproduce these characteristics. For CT-CT-OS-CS type torsions, the values of 0.383 for V3 and 0.1 for V1 with a 180° shift agree with *ab initio* results. This profile is the same as that of the current CT-CT-OS-CT torsion in the AMBER database. CT-OS-CS-CS and CS-CS-OS-CE torsions had a slight modification to these values, with V3 set at 1.50 and V1 set at 0.3 with a 180° shift. While these values give excellent agreement for the low energy conformers, they do increase the barriers between conformations slightly. To test the effect on these barriers, alternative parameters of V3 = 0.1 and V1 = 0.1 with a 180° shift were evaluated. These values would give a much more flexible side chain, with lower barriers and a smaller difference between low energy conformers. In the actual molecular dynamics simulations, however, both sets of parameters gave essentially identical results, with the same distribution profile for the side chains. The OS-CS-CS-OS torsion was reproduced by using a value of 1.00 for V2. All of the new parameters necessary for simulation of 2′-substituted *O*-(2-methoxyethyl) side chains are reported in Table 2.

Table 2. Force field parameters for MOE simulations

Bonds:	r_{eq}, Å	K_r, kcal/(mol Å^2)
CS-CS	1.526	310.0
CE-H1	1.090	340.0
CS-H1	1.090	340.0
CE-OS	1.410	320.0
CS-OS	1.410	320.0
Angles:	θ_{eq}	K_θ, kcal/(mol rad^2)
CS-CS-H1	109.50	50.0
CS-CS-OS	109.50	50.0
H1-CE-H1	109.50	35.0
H1-CS-H1	109.50	35.0
H1-CE-OS	109.50	50.0
H1-CS-OS	109.50	50.0
CE-OS-CS	109.50	60.0
CT-OS-CS	109.50	60.0

Torsions:	# of paths	$V_n/2$ [a]	γ [b]	n [c]
X -CS-CS-X	9	1.40	0.0	3
X -CE-OS-X	3	1.15	0.0	3
X -CS-OS-X	3	1.15	0.0	3
CT-CT-OS-CS	1	0.383	0.0	3
CT-CT-OS-CS	1	0.1	180.0	2
CS-CS-OS-CE	1	1.50	0.0	3
CS-CS-OS-CE	1	0.30	180.0	1
CT-OS-CS-CS	1	1.50	0.0	3
CT-OS-CS-CS	1	0.30	180.0	1
OS-CS-CS-OS	1	1.00	0.0	2

[a]Magnitude of torsion in kcal/mol.
[b]Phase offset in degrees.
[c]Periodicity of the torsion.

SIMULATIONS

Methods

Molecular dynamics calculations were performed on the sequence MOE[CCAACGTTGG]-r[CCAACGUUGG]. The starting structure was based on canonical Arnott A-form geometry generated with the NUCGEN module of the AMBER 4.1 package. New residues for the MOE-containing residues were created with the PREP module and matched to the starting A-form geometry. System neutrality was achieved by placing 18 Na^+ counterions around the phosphate backbone with the EDIT module. The entire duplex was surrounded by a 9 Å shell of TIP3P water molecules (2895 water molecules, box dimensions 60 × 45 × 41 Å).

The water and counterions were energy minimized to a gradient of <0.1 kcal/mol Å and then allowed to equilibrate for 10 ps molecular dynamics. After the initial equilibration, the entire system was minimized to an energy gradient of <0.1 kcal/mol Å. Constrained molecular dynamics were then initiated on the complete system. Initial velocities for all atoms were assigned from a Maxwellian distribution around 300 K. For this and all subsequent simulations, a time step of 2 fs was used with the SHAKE algorithm (26) to constrain bonds containing hydrogen atoms. The pressure was held constant at 1.0 atm and the temperature was held constant at 300 K using the Berendson coupling method (27). Non-bonded interactions were updated every 20 steps of dynamics, with the Particle Mesh Ewald (PME) technique (19) used for the treatment of electrostatic interactions. Molecular dynamics calculations were initiated with 10.0 kcal/mol constraints on all atoms of the duplex. After 20 ps, this was decreased to 1.0 kcal/mol, and then to 0.1 kcal/mol after another 20 ps, for a total of 60 ps of constrained dynamics. After this equilibration period, all constraints were removed and collection runs were initiated. Simulations were carried out for a total run of 1 ns. Analysis of the trajectory was performed using the CARNAL module of AMBER.

Results and Discussion

The MOE[CCAACGTTGG]-r[CCAACGUUGG] duplex was started with an A-form geometry and retained this general form for the duration of the simulation. The RMS deviation (RMSD) from the A-form starting structure is quite low for the duration of the simulation, with an average RMSD of 2.0 Å (Fig. 3a). Figure 3b shows the minor groove width, which is ~15.5 Å between P atoms (versus 17 Å for A-form and 13 Å for B-form). The distance between intra-strand phosphate atoms (Fig. 3c) is ~6 Å (versus 5.65 Å for A-form and 6.55 Å for B-form). The most convincing A-form type feature is the average sugar pucker, which is C3′ *endo* (northern) for all residues in both strands. Figure 3d shows

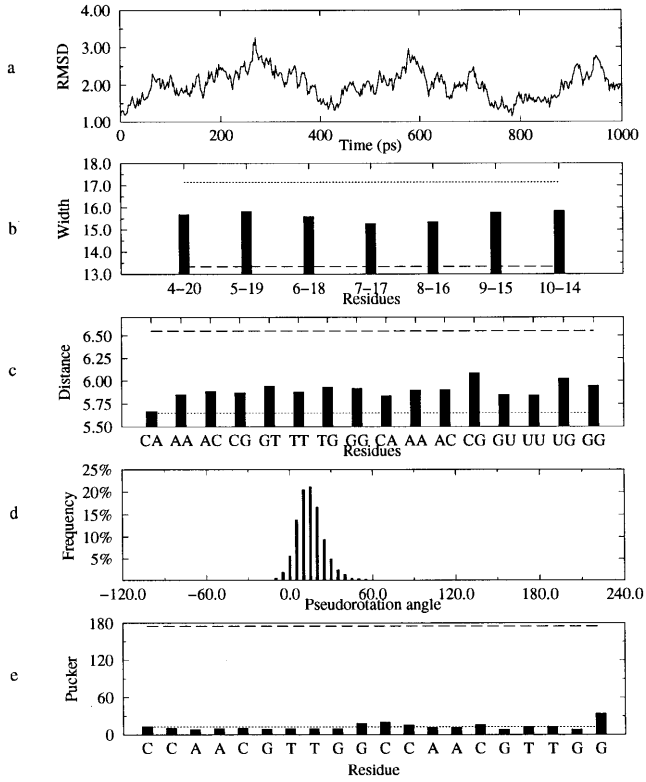

Figure 3. Results from molecular dynamics simulation. (**a**) RMSD from canonical A-form geometry. (**b**) Distance between phosphate atoms across the minor groove. (**c**) Distance between phosphate atoms in the same strand. (**d**) Distribution of sugar pucker pseudorotation angles. (**e**) Average sugar pucker for each residue. Dotted lines represent canonical A-form values, dashed lines represent canonical B-form values.

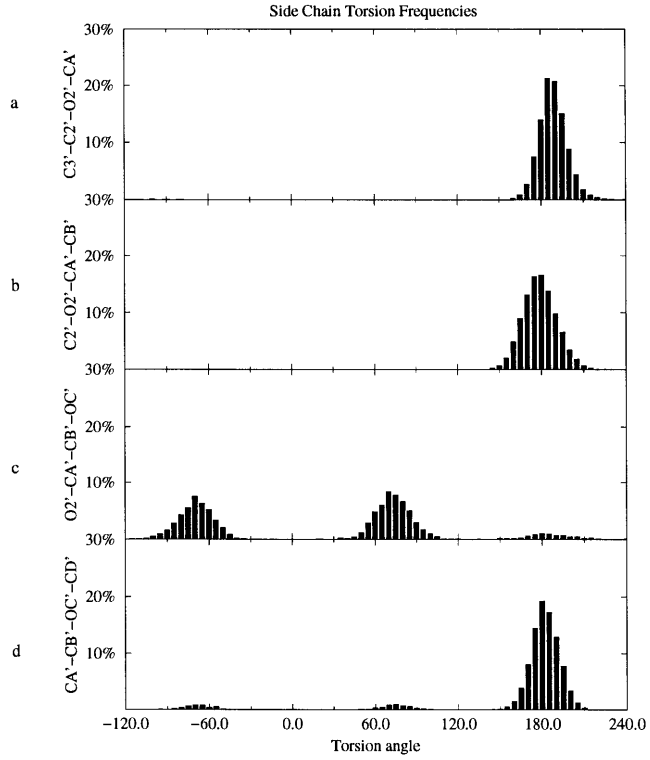

Figure 4. Distribution of torsion angles around 2′-*O*-(2-methoxyethyl) side chains. (**a**) C3′-C2′-O2′-CA′; (**b**) C2′-O2′-CA′-CB′; (**c**) O2′-CA′-CB′-OC′; (**d**) CA′-CB′-OC′-CD′.

that the distribution of sugar puckers falls at ~10° for the entire simulation and Figure 3e shows that the average sugar pucker pseudorotation angle for each residue is ~10°. All of these characteristics are sustained for the duration of the simulation and there are no periods when the duplex does not have an overall A-form type geometry. These features are also seen in the crystallographic structure of the MOE-substituted duplex d[GCGTAT$_{MOE}$ACGC]$_2$ (17). The average pseudorotation angle of all sugars in the crystal structure is 10°, which is consistent with an A-form geometry. Phosphate distances are nearly identical to those of the simulated structure, with the minor groove width being 16 Å and the intra-strand distances being 6 Å. Comparing the crystal structure to our own shows a very similar overall shape, with an RMSD of only 2.0 Å between the sugar phosphate backbones (data not shown).

The 2′-*O*-(2-methoxyethyl) side chain itself also has a relatively stable geometry within the duplex. The three lowest energy conformations from the parameterization are seen during the molecular dynamics simulations, however, the *trans*/*gauche*/*trans* conformer is by far the most predominant. The infrequent occurrence of the *trans*/*trans*/*trans* geometry may be a result of the higher dielectric field of the solvent, which, as noted in the parameterization section, will affect the relative energies of the different conformers. The C3′-C2′-O2′-CA′ and C2′-O2′-CA′-CB′ torsions are both *trans* (180°) in all residues for the duration of the simulation. The O2′-CA′-CB′-OC′ torsion has more flexibility, but adopts either a *gauche*+ or *gauche*– (±60°) angle during the simulation. The end CA′-CB′-OC′-CD′ torsion is generally *trans*, with short periods of *gauche* conformations. Figure 4 shows the distribution of each of these torsions from all residues for the duration of the simulation.

The two substituted residues in the crystal structure have similar torsion angles to those of the simulated sequence. The C3′-C2′-O2′-CA′ and C2′-O2′-CA′-CB′ torsions are again *trans* for both residues containing the modification. The O2′-CA′-CB′-OC′ torsion is *gauche*– for both residues (–37° and –49°), which is seen in the simulated structure half of the time. The biggest difference from the simulated structure is seen in the end CA′-CB′-OC′-CD′ torsion, which is *gauche*– in both residues (–70° and –85°), as opposed to predominantly *trans* for the simulated structure. This *trans*/*gauche*–/*gauche*– conformation was found to be 2 kcal higher in energy than the extended all-*trans* conformer during the parameterization, however, it is again likely that this conformer has a much lower relative energy in solution. It is interesting to note that this conformation is seen very infrequently during the dynamics simulation of the duplex. This small structural difference may be a result of the substitution patterns studied or due to the conditions used in determining the crystal structure. It is important to mention that the simulated structure has all 2-methoxyethyl substitutions on one strand when the target strand is RNA. This causes the side chains to rotate in the same direction in the minor groove, to avoid colliding with each other. Each end methyl group is rotated out so that it faces away from the groove and into the solvent. In contrast, the crystal structure is composed of DNA residues with only two substitutions, which are directly opposite from each other across the minor

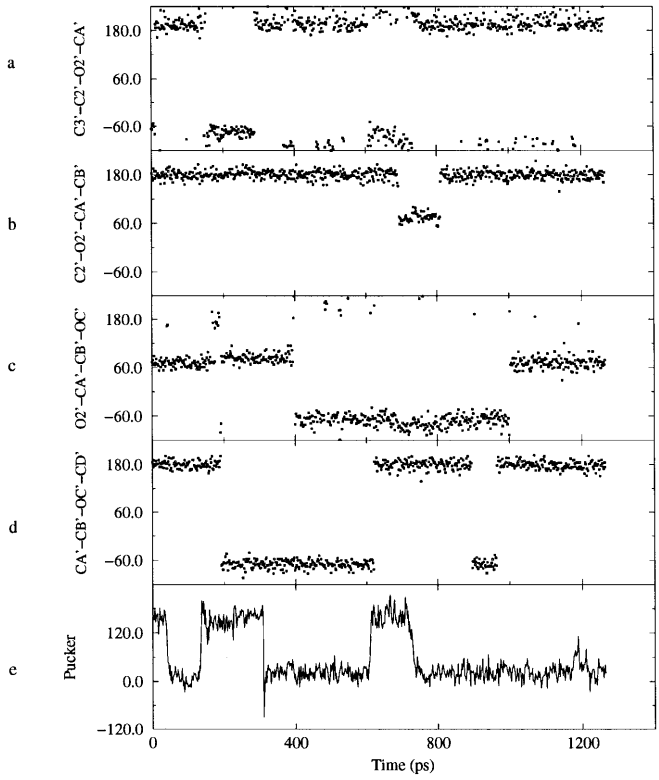

Figure 5. Single MOE-guanosine residue results for the duration of the simulation. (**a**) Sugar pucker; (**b**) C3′-C2′-O2′-CA′ torsion; (**c**) C2′-O2′-CA′-CB′ torsion; (**d**) O2′-CA′-CB′-OC′ torsion; (**e**) CA′-CB′-OC′-CD′ torsion.

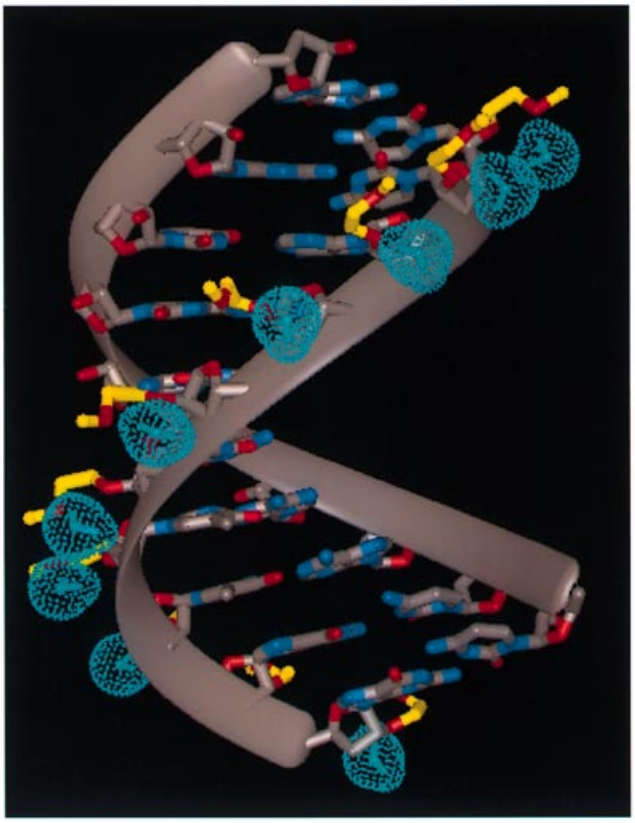

Figure 6. MOE[CAACGTTGG]-r[CCAACGUUGG] duplex and water molecules within 2.0 Å of the MOE side chain at the end of a 1 ns simulation.

groove. The end methyl group in this case is rotated toward the adjacent 3′-sugar and appears to interact with the C4′ and C5′ atoms of this sugar. A *trans* rotation around the CB′-OC′ bond (such as seen in the simulated structure) may be less favorable, as it would place the ends of the two side chains in somewhat closer proximity to each other.

To understand more about the nature of the MOE substitution, we performed a 1.2 ns simulation of a single MOE-guanosine utilizing the same methods as in the duplex simulation. In comparing the dynamic properties of the duplex and nucleoside, the MOE side chain appears more flexible in the single nucleoside than in the duplex. The MOE-nucleoside adopts both the *trans*/*gauche*/*trans* and the *trans*/*gauche*–/*gauche*– conformations. This suggests that the duplex in water may have different stereochemical requirements for the side chain rotation, possibly solvent mediated. Figure 5a–d shows the values of each side chain torsion throughout the trajectory. Figure 5e also shows the sugar pucker of the nucleoside during the simulation. At 100 ps the guanine base undergoes a natural rotation from the *anti* conformation to the *syn* conformation, which allows C2′ *endo* puckering to occur. However, by constraining the glycosidic torsion to the *anti* conformation (which is the only conformer in duplexes), the C3′ *endo* pucker becomes favored and predominates for the remainder of the simulation. This preference is in concert with NMR and CD results that show 2′-*O*-alkyl substitutions favor a C3′ *endo* sugar pucker and an overall A-form geometry (3,14).

The simulations also reveal that the MOE side chains may have a direct interaction with water molecules solvating the duplex. The oxygen atoms, especially in the MOE side chain, appear capable of forming a water-mediated interaction with the 3′-oxygen of the phosphate backbone. The presence of the two oxygen atoms in the MOE side chain and the *gauche* rotation around the O-C-C-O torsion creates a very electronegative groove that is a likely binding site for water molecules. Throughout the simulation a number of different water molecules are observed to occupy a position in this groove within hydrogen bonding distance of both the OC′ side chain atom and O3′ backbone atom. Figure 6 shows this groove and the water molecules associated with it at the end of the 1 ns simulation. The crystal structure also has one water molecule bound in this ‘mini’ groove of each MOE residue. The presence of these water molecules may play a role in holding the side chains in the preferable *gauche* conformation.

CONCLUDING REMARKS

This study has explored the structural and dynamic features of a 2′-*O*-(2-methoxyethyl)-substituted nucleic acid complex in aqueous medium. Overall, the results show that the simulated duplex adopts an A-form conformation that is remarkably similar to that of a DNA:DNA crystal structure containing a single MOE substitution at the middle position. While sequence-specific effects cannot be entirely ruled out, the analysis presented here, as well as other work on 2′-substituted nucleic acids (28,29), suggests that this conformational preference is driven by the MOE substitution, which favors C3′ *endo* puckering. In comparing MOE side chain conformations in the simulated and crystallo-

graphic structures, minor differences are seen primarily in the rotation of the end methyl group, which appears to adopt a more extended form in solution. This may be due, in part, to sequence-specific effects or, more likely, to differences in the conditions in the crystallographic and solution phases (which in turn produce structural effects). A close examination of the crystal structure shows that a potential hydrophobic contact between the end methyl group and the adjacent sugar may drive this more compact, *gauche* rotation of the MOE side chain. This contact, however, does not appear possible in the solution phase form.

When evaluating the stability of the MOE-substituted duplex, it is important to note that A-form structures are more stable than either B-form or hybrid complexes. By adopting the A-form geometry, the bases are aligned for more stable π–π interactions from base stacking. The preference for an A-form geometry may account for some of the improved binding affinity of MOE-substituted duplexes, but does not explain the improved stability seen compared with natural RNA:RNA duplexes. The *O*-(2-methoxyethyl) side chain itself must impart some additional stability to the duplex. This is most likely a result of an entropic advantage due to pre-organization of the MOE-substituted strand. A simulated four residue MOE-substituted single strand appears to have a rigid structure that is very similar to the MOE strand of the duplex. In contrast, a single strand of natural DNA or RNA appears to have a more random character that would be entropically advantageous. Substitution with the MOE side chain removes any entropic gain that would occur upon denaturation to a single strand. This entropic difference explains the increase in stability for MOE-substituted duplexes relative to RNA and DNA duplexes.

A related item is the entropy for solvation of the duplex versus that of the two single strands. Formation of two single strands requires ordering of several additional water molecules and is entropically unfavorable. In the MOE strand the O2′ and CA′ atoms of the side chain are relatively inaccessible to water molecules in the duplex. Hydration of this portion in a single strand would require ordering of several additional water molecules beyond those of normal DNA or RNA, which would incur an additional entropic cost. Any 2′-*O*-alkyl-substituted oligonucleotide would pay this penalty for formation of a single strand, which would contribute to an increase in stability of the duplex. However, the flexible alkyl chain would require ordering of itself in the duplex, which would counter this increased stability. Small substituents, such as the 2′-*O*-methyl side chain, would remain organized in both states, while longer side chains would require more ordering upon hybridization. This may relate to the correlation between increasing 2′-*O*-alkyl chain length and decreasing duplex stability. The MOE side chain is unique, as it is highly organized, resulting in little difference in entropy for the substituent in a single strand or duplex. Essentially, the pre-organized MOE side chain requires ordering of additional water molecules when in the single strand, while it remains stable and does not change. Desolvation of these water moleculess upon hybridization leads to the increased stability of the duplex.

A final possibility is related to enthalpic contributions to hydration of the duplex. RNA duplexes are more extensively hydrated than DNA, which is primarily due to the presence of the 2′-hydroxyl group. RNA does pay an entropic penalty for ordering these water molecules, however, this cost is overcome by an enthalpic gain from the network of hydrogen bonds between the two strands. Any 2′ substitution would have a direct effect on this water shell. A 2′-*O*-alkyl chain could maintain a portion of the network due to the hydrogen bond-accepting character of the oxygen atom, however, the flexible hydrophobic alkyl portion would disrupt some of the network. Again, smaller substituents would have less of an impact, while longer side chains would disturb the shell more. The *gauche* rotation around the O-C-C-O torsion of the 2′-*O*-(2-methoxyethyl) substitution effectively locks the side chain in a conformation that has very little interference with the minor groove. Because the bulk of the side chain is rotated away from the minor groove, the MOE substituent will not disrupt the water shell, but will be allowed to participate in the stabilizing hydrogen bond network.

ACKNOWLEDGEMENTS

We would like to thank Professor Martin Egli for providing a preprint of his paper detailing the crystal structure of a MOE-substituted duplex. K.E.L. would like to acknowledge support from NIH Training Grant GM07994. We would also like to thank the National Cancer Institute for allocation of computing time and staff support at the Frederick Biomedical Supercomputing Center.

REFERENCES

1 Crooke,S.T. (1996) *Med. Res. Rev.*, **16**, 319–344.
2 De Mesmaeker,A., Haner,R., Martin,P. and Moser,H.E. (1995) *Acc. Chem. Res*., **28**, 366–374.
3 Saenger,W. (1984) *Principles of Nucleic Acid Structure*. Springer-Verlag, New York, NY.
4 Lesnik,E.A. and Freier,S.M. (1995) *Biochemistry*, **34**, 10807–10815.
5 Conte,M.R., Conn,G.L., Brown,T. and Lane,A.N. (1997) *Nucleic Acids Res*., **25**, 2627–2634.
6 Searle,M.S. and Williams,D.H. (1993) *Nucleic Acids Res*., **21**, 2051–2056.
7 Egli,M., Portmann,S. and Usman,N. (1996) *Biochemistry*, **35**, 8489–8494.
8 Lane,A.N., Ebel,S. and Brown,T. (1993) *Eur. J. Biochem*., **215**, 297–306.
9 Fedoroff,O.Y., Salazar,M. and Reid,B.R. (1993) *J. Mol. Biol*., **233**, 509–523.
10 Gonzalez,C., Stec,W., Reynolds,M.A. and James,T.L. (1995) *Biochemistry*, **34**, 4969–4982.
11 Horton,N.C. and Finzel,B.C. (1996) *J. Mol. Biol*., **264**, 521–533.
12 Baker,B.F., Lot,S.L., Condon,T.P., Cheng-Flournoy,S., Lesnik,E.A., Sasmor,H.M. and Bennett,C.F. (1997) *J. Biol. Chem*., **272**, 11944–12000.
13 Freier,S.M. and Altmann,K. (1997) *Nucleic Acids Res*., **25**, 4429–4443.
14 Lesnik,E.A., Guinosso,C.J., Kawasaki,A.M., Sasmor,H., Zounes,M., Cummins,L.L., Ecker,D.J., Cook,P.D. and Freier,S.M (1993) *Biochemistry*, **32**, 7832–7838.
15 Wolfe,S. (1972) *Acc. Chem. Res*., **5**, 102.
16 Abe,A. and Mark,J. (1976) *J. Am. Chem. Soc*., **98**, 6468.
17 Tereshko,V., Portmann,S., Tay,E.C., Martin,P., Natt,F., Altman,K. and Egli,M. (1998) *Biochemistry*, in press.
18 Cornell,W.D., Cieplak,P., Bayly,C.I., Gould,I.R., Merz,K.M., Ferguson,D.M., Spellmeyer,D.C., Fox,T., Caldwell,J.W. and Kollman,P.A. (1995) *J. Am. Chem. Soc*., **117**, 5179–5197.
19 Essman,U., Perera,L., Berkowitz,M.L., Darden,T., Lee,H. and Pedersen,L.G. (1995) *J. Am. Chem. Soc*., **103**, 8577–8593.
20 Cieplak,P., Cornell,W.D., Bayly,C. and Kollman,P.A. (1995) *J. Comp. Chem*., **16**, 1357–1377.
21 Frisch,M.J., Trucks,G.W., Schlegel,H.B., Gill,P.M.W., Johnson,B.G., Robb,M.A., Cheeseman,J.R., Keith,T., Petersson,G.A., Montgomery,J.A. *et al*. (1995) *Gaussian 94*, Revision D.2. Gaussian Inc., Pittsburgh, PA.
22 Pearlman,D.A., Case,D.A., Caldwell,J.W., Ross,W.R., Cheatham,T.E., Ferguson,D.M., Seibel,G.L., Singh,U.C., Weiner,P.K. and Kollman,P.A. (1995) *AMBER 4.1*. University of California, San Francisco, CA.
23 Jaffe,R.L., Smith,G.D. and Yoon,D.Y. (1993) *J. Phys. Chem*., **97**, 12745–12751.
24 Abe,A., Tasake,K. and Mark,J.E. (1985) *Polymer J*., **17**, 883.
25 Tasaki,K. and Abe,A. (1985) *Polymer J*., **17**, 641.
26 Ryckaert,J.P., Ciccotti,G. and Berendsen,H.J.C. (1977) *J. Comp. Phys*., **23**, 327–341.
27 Berendsen,H.J.C., Postma,J.P.M., van Gunsteren,W.F., DiNola,A. and Haak,J.R. (1984) *J. Comp. Phys*., **81**, 3684–3690.
28 Egli,M., Usman,N. and Rich,A. (1993) *Biochemistry*, **32**, 3221.
29 Ban,J., Ramakrishnan,B. and Sundaralingam,M. (1994) *J. Mol. Biol*., **236**, 275.